

Characterisation of a ^{90}Sr based electron monochromator

S. Arfaoui*, C. Joram*, C. Casella†

* *CERN, Switzerland*

† *Institute for Particle Physics, ETH Zurich, Switzerland*

May 6, 2015

Abstract

This note describes the characterisation of an energy filtered ^{90}Sr source to be used in laboratory studies that require Minimum Ionising Particles (MIP) with a kinetic energy of up to ~ 2 MeV. The energy calibration was performed with a LYSO scintillation crystal read out by a digital Silicon Photomultiplier (dSiPM). The LYSO/dSiPM set-up was pre-calibrated using a ^{22}Na source. After introducing the motivation behind the usage of such a device, this note presents the principle and design of the electron monochromator as well as its energy and momentum characterisation.

1. Introduction

In the context of calorimetry R&D for future linear collider experiments, several technologies are currently under study within the CALICE [1] collaboration, all of them aiming at unprecedented highly granular segmentations to be used with particle flow algorithms [2].

In particular, an electromagnetic calorimeter based on small plastic scintillators coupled to silicon photomultipliers (SiPM) has been proposed. A study has been started at CERN on the characterisation of the light yield and its uniformity of small plastic scintillators, of sizes ranging from $10 \times 10 \times 2 \text{ mm}^3$ to $30 \times 30 \times 5 \text{ mm}^3$. These characterisations are performed using various light containment solutions, such as wrapping the scintillator with an Enhanced Specular Reflective¹⁾ (ESR) foil or painting its faces with a reflector paint²⁾.

To produce the scintillation light in such laboratory set-ups, electron sources are generally used, in particular the β emitting ^{90}Sr isotope, which in combination with the decay of the daughter nucleus Y-90 provides a continuous electron energy spectrum extending up to $\sim 2.2 \text{ MeV}$, as shown in Fig. 1.

In order to properly quantify the yield and uniformity of the scintillator under test, it is important to have knowledge of the amount of energy deposited by the traversing electrons. This can be achieved by the use of Minimum Ionising Particles (MIPs). Fig. 2 (top) shows the stopping power (dE/dx) of electrons in a polyvinyltoluene-based plastic scintillator. The lower plot shows the corresponding range. The density of plastic scintillator is 1.03 g/cm^3 . Both plots were generated by the ESTAR program provided by NIST³⁾

Electrons above $\sim 1 \text{ MeV}$ can be considered MIPs and will traverse scintillating tiles of few mm thickness as under study for the ECAL application. Therefore, the goal is to prevent elec-

¹⁾3M ESR

²⁾Saint-Gobain BC-620

³⁾NIST ESTAR <http://physics.nist.gov/PhysRefData/Star/Text/ESTAR.html>

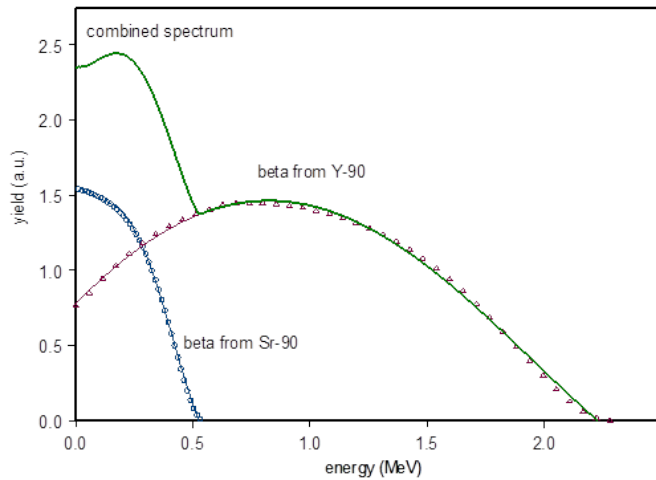


Figure 1: β spectrum of ^{90}Sr and the daughter nucleus ^{90}Y .

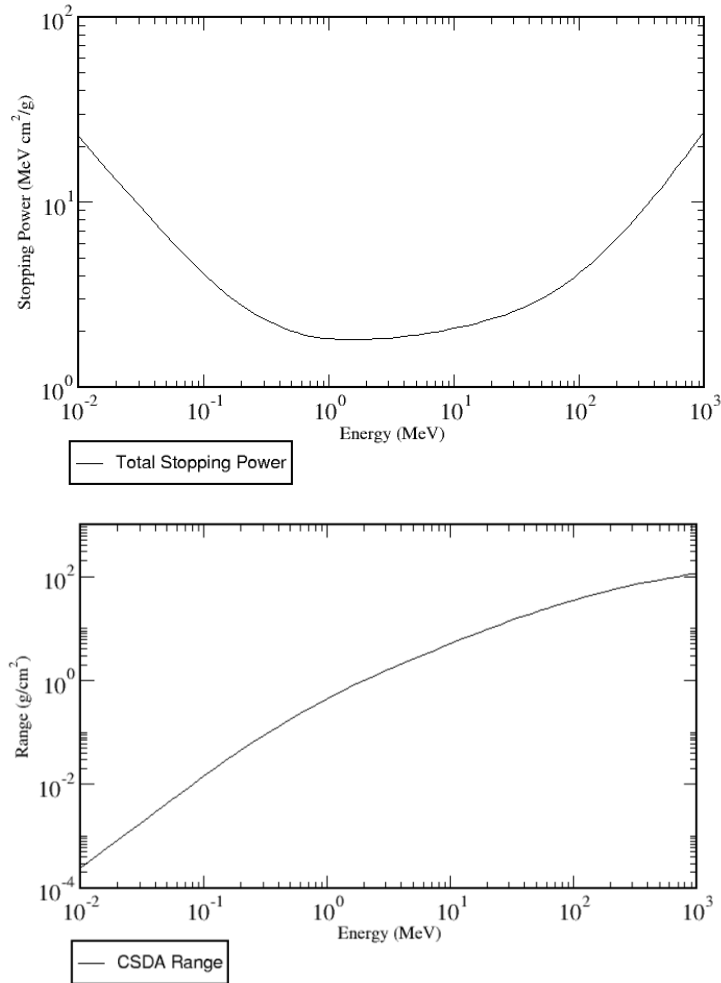


Figure 2: Top: Stopping power (dE/dx) of electrons in a polyvinyltoluene-based plastic scintillator. Bottom: Range of electrons in the same material. The x-axis corresponds to the kinetic energy of the electrons.

trons of lower energy from reaching the scintillator under test, which can be done by selecting the electron momentum using a magnetic field.

The following section briefly describes how such a solution is implemented in the form of a compact electron monochromator.

2. The electron monochromator

The device described here is based on the original design by the *Institut de Recherches Subatomiques*, Strasbourg, France. From their technical drawings, shown in Appendix B, the manufacturing of the tungstene pieces was externally contracted, all other components were fabricated

at CERN. The ^{90}Sr source itself was inserted by CERN's radio-protection group.

The electron monochromator, illustrated on Fig. 3 consists of three main parts. The body is made of tungsten which ensures efficient shielding in all directions. The source housing, which contains the $\sim 350\text{ MBq } ^{90}\text{Sr}$ source, is also made of tungsten and is permanently bolted to the side of the main body. A collimated hole is present inside the source housing pointing inwards, allowing the electrons to escape. The solenoid coil, mounted on top of the main body, is made of 16 layers of 0.80 mm coated copper wires, arranged in 56 windings per layer. Moreover, the coil is equipped with an ARMCO soft iron core to enhance the generated magnetic field. A cavity inside the main body allows the electrons to travel from the source casing and, in the presence of a magnetic field, bend towards the exit hole on the bottom side of the body. The magnetic field is guided to the cavity via soft iron bars on the sides and additional soft iron cylinders on the level of the cavity.

When no current is applied to the solenoid, the electrons exiting the source casing are stopped inside the tungsten structure, allowing for safe operation and handling of the device. A small Hall probe allowed to measure the magnetic field in between the two soft iron cylinders as a function of the magnet current. The result is shown in the upper plot of Fig. 4. Dismantling and re-assembly of the source (with the ^{90}Sr - source removed) showed that the current-field relation changed. This is due to the fact that the width of the air gaps between the various soft iron pieces depend on the applied torque to the screws. For relatively high fields (several thousand Gauss) the air gaps lead to losses. It was however demonstrated that the relation between relative rate and actual magnetic field, as shown in the lower plot of Fig. 4, is not affected.

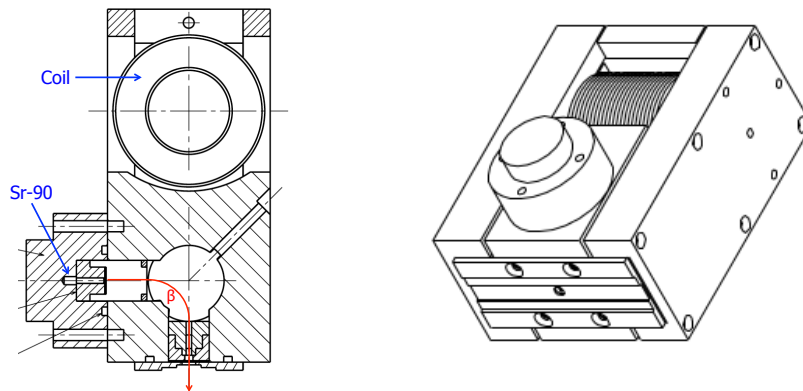


Figure 3: Technical drawings of the electron monochromator. The solenoid coil and the ^{90}Sr tungsten casing can be seen. When a current is applied to the coil, the electrons are deviated to the collimated opening on the bottom.

Overall dimensions: $130 \times 100 \times 60\text{ mm}$.

Proper use of the device requires to know the relation between the solenoid current (or the magnetic field in between the soft iron cylinders) and the electron momentum, as well as the spread of the selected momenta. The following sections describe how the electron monochromator was characterised using a LYSO crystal coupled to a dSiPM.

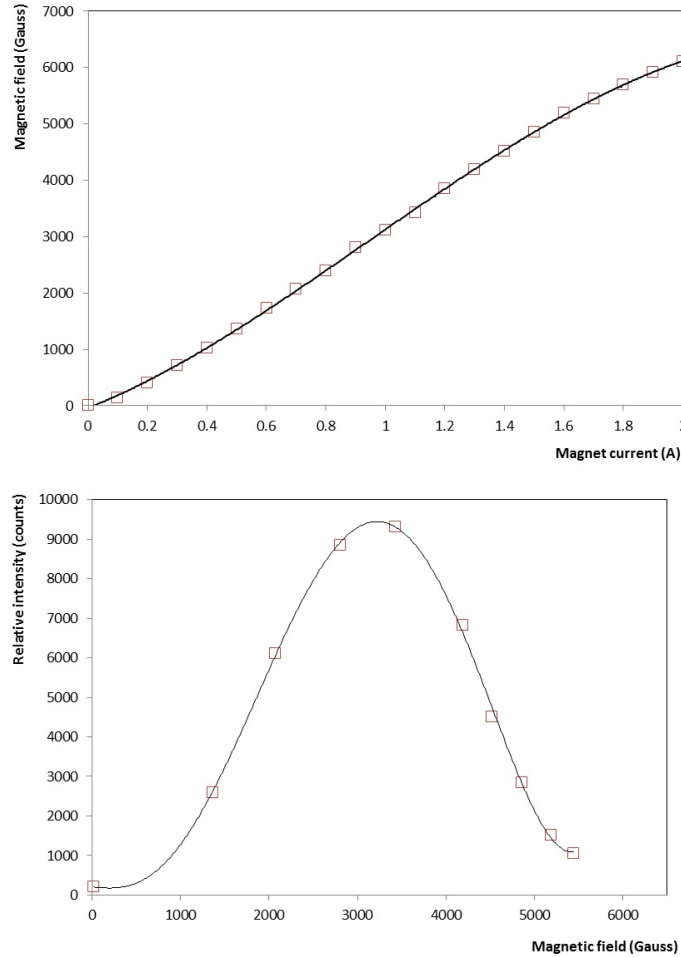


Figure 4: Top: The magnetic field in between the two soft iron cylinders is plotted versus the applied magnet current. Bottom: The relative intensity at the output of the monochromator is plotted versus the magnetic field. The measurement has been performed with plastic scintillators. The counts are collected in typically 100 s.

3. Experimental set-up

The AX-PET collaboration [3] has developed a PET demonstrator [4] based on axially arranged layers of scintillator crystals read out with conventional analogue silicon photomultipliers (SiPM). In a second phase, an alternative readout has been studied [5] using digital silicon photomultipliers (dSiPM) [6] developed by Philips.

One of these dSiPM arrays, coupled to a LYSO crystal, has been used to characterise the electron monochromator. The dSiPM array used has a surface $32 \times 32 \text{ mm}^2$, and its type is DPC-6400-22-44. It consists of 16 *dies* ($7.15 \times 7.9 \text{ mm}^2$), each segmented into 4 *pixels*. Each $3.2 \times 3.9 \text{ mm}^2$ pixel is comprised of a matrix of 6400 avalanche photo-diodes operated in Geiger

mode, each capable of detecting single photons. Details on the operation of the dSiPM can be found in [5].

The LYSO crystal, $3 \times 3 \times 3 \text{ mm}^3$ in size, is coated with a TiO_2 reflective paint on 5 of its sides in order to improve light containment. The bare face is glued to one of the dSiPM pixels, effectively covering $\sim 72\%$ of its surface. Therefore, only ~ 4600 of the 6400 cells are exposed to the light of the crystal.

Before characterising the electron monochromator, a calibration of the non-linear response of the LYSO/dSiPM arrangement is required. This is performed by comparing the dSiPM amplitude, *i.e.* the number of dSiPM cells fired, to the known energies of the photons emitted by a ^{22}Na source. The experimental set-up for this non-linearity measurement, sketched in Fig. 5, consists of the following elements:

- a ^{22}Na source for the dSiPM + LYSO calibration
- the dSiPM array and its readout electronics
- the LYSO crystal, glued to the dSiPM array
- a laptop for the dSiPM readout

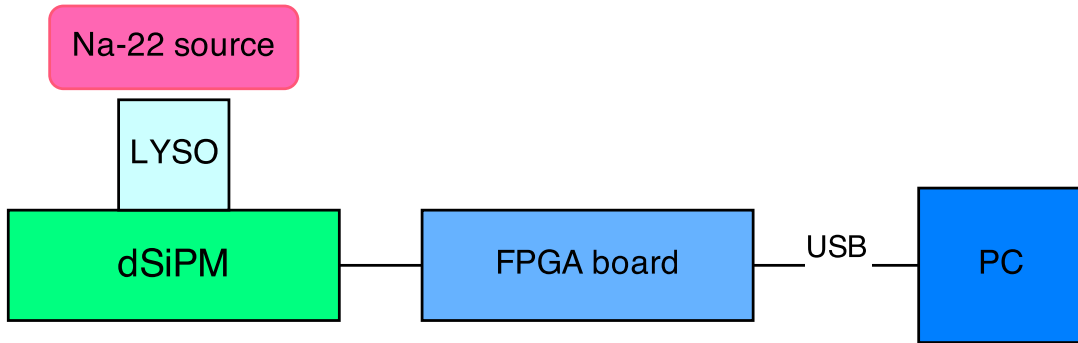


Figure 5: Schematic representation of the experimental set-up for measuring the non-linearity of the LYSO/dSiPM arrangement.

The results of the calibration are shown in the following section.

4. dSiPM calibration

The number of dSiPM cells fired for a given energy deposit E in the LYSO crystal can be written as follows:

$$N_{cells} = \alpha \cdot \left[1 - \exp\left(-\frac{E}{\beta}\right) \right] \quad (1)$$

where α and $p\beta$ are calibration constants. This functional relation reflects the signal saturation imposed by the combinatorics due to the finite number of dSiPM cells (4600). A cell which is hit by two and more photons is still only counted as 1 hit. To determine the calibration constants, the LYSO was exposed to a ^{22}Na source as shown on Fig. 5 and a dSiPM response spectrum was acquired; it is shown in Fig. 6 (left). The two main peaks correspond to the positronium annihilation, resulting in two photons of 511 keV, and a nuclear transition line at 1270 keV, respectively. They were both fitted with a Gaussian distribution and their mean values, together with the origin (0,0) appear on the graph of Fig. 6 (right). This graph was fitted with the function shown on Eq. 1 and the parameters α and β were obtained.

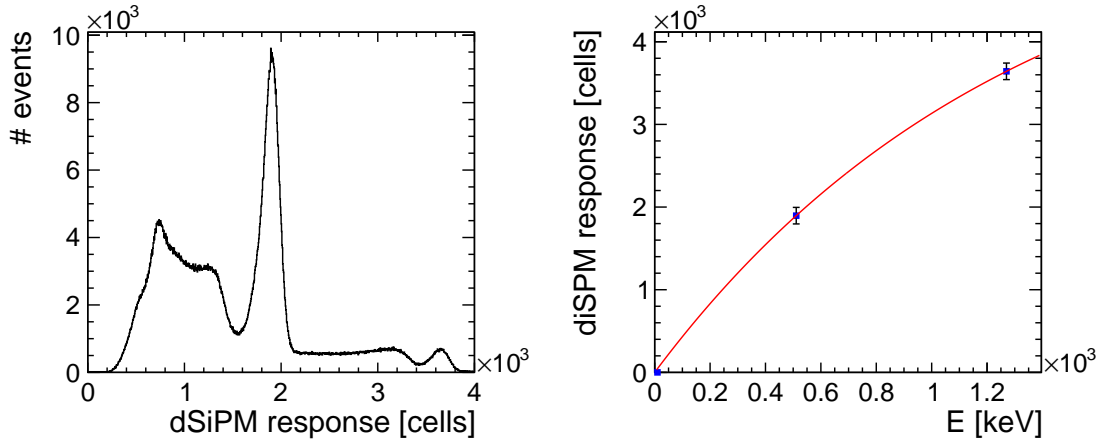


Figure 6: Left: Spectrum of the number of dSiPM cells fired under the ^{22}Na source, showing the 511 keV positronium annihilation peak, the 1.27 MeV nuclear transition peak, and their respective Compton edges. Right: Calibration fit using the identified peaks, including the point corresponding to $(E = 0 \text{ keV}; N_{\text{cells}} = 0)$.

Using the relation between the numbers of dSiPM cells fired and the energy deposited in the LYSO crystal, it is now possible to characterise the electron monochromator in energy and momentum, as detailed in the next section.

5. Electron monochromator characterisation

The experimental set-up, sketched in Fig. 7, is similar to the calibration with the ^{22}Na source, however now the ^{90}Sr β source is being used. The electron monochromator exit hole was placed above the LYSO crystal, as close as possible. The procedure was to set various solenoid currents and for each, acquire a dSiPM response spectrum.

The number of fired dSiPM cells, N_{cells} , can be converted into an energy deposit using the previously obtained calibration:

$$E = -\beta \cdot \ln \left(1 - \frac{N_{\text{cells}}}{\alpha} \right) \quad (2)$$

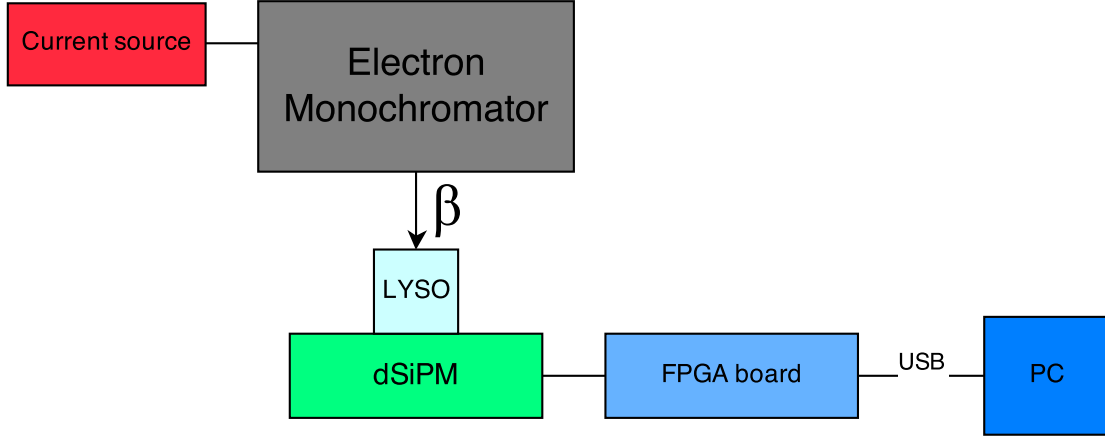


Figure 7: Schematic representation of the experimental set-up for the energy calibration of the electron monochromator.

and the momentum p can be calculated as follows:

$$p = \sqrt{(E + m_e)^2 - m_e^2} \quad (3)$$

where $m_e = 511$ keV is the electron mass.

Fig. 8 shows an example momentum spectrum obtained at a solenoid current of 1.2 A. Distributions for other current setting can be found in Appendix A. The main peak corresponds the electrons passing the monochromator. This peak moves linearly with the settings of the solenoid current. The background does not depend on the magnetic field inside the monochromator and is attributed to bremsstrahlung photons (soft X-rays) that are produced by electrons inside the steel/tungsten casing. While these X-ray photons are visible in the high-Z LYSO crystals, the Z^{4-5} dependence of the photoelectric effect would suppress their detection in a plastic scintillator.

Table 1 summarises the results of the full measurement campaign, showing the observed number of dSiPM cells fired, the calculated energies, momenta, and respective resolutions for each setting of the solenoid current. Below 0.4 A, no peak was visible above the bremsstrahlung background. Beyond 1.6 A, the end of the ^{90}Sr β -emission spectrum is being approached, and the rate decreases rapidly. The precision of the momentum selection is generally better than 10%, for momenta above 1.5 MeV/c it approaches 5%.

In order to verify the expected linearity between the electron momentum and the solenoid current, each value was added to a graph fitted with a first degree polynomial, as shown in Fig. 9. A good linearity is observed over the current range explored. Finally, Fig. 10 shows the energy and momentum selection resolutions as a function of the solenoid current. We observe that a momentum selection resolution of $\sim 5\%$ can be achieved for currents above 1.4 A. This solenoid current value corresponds to our working point for MIP selection in our 2 mm thick scintillator studies.

It should be noted that, as described above, the relation between the magnet current and the

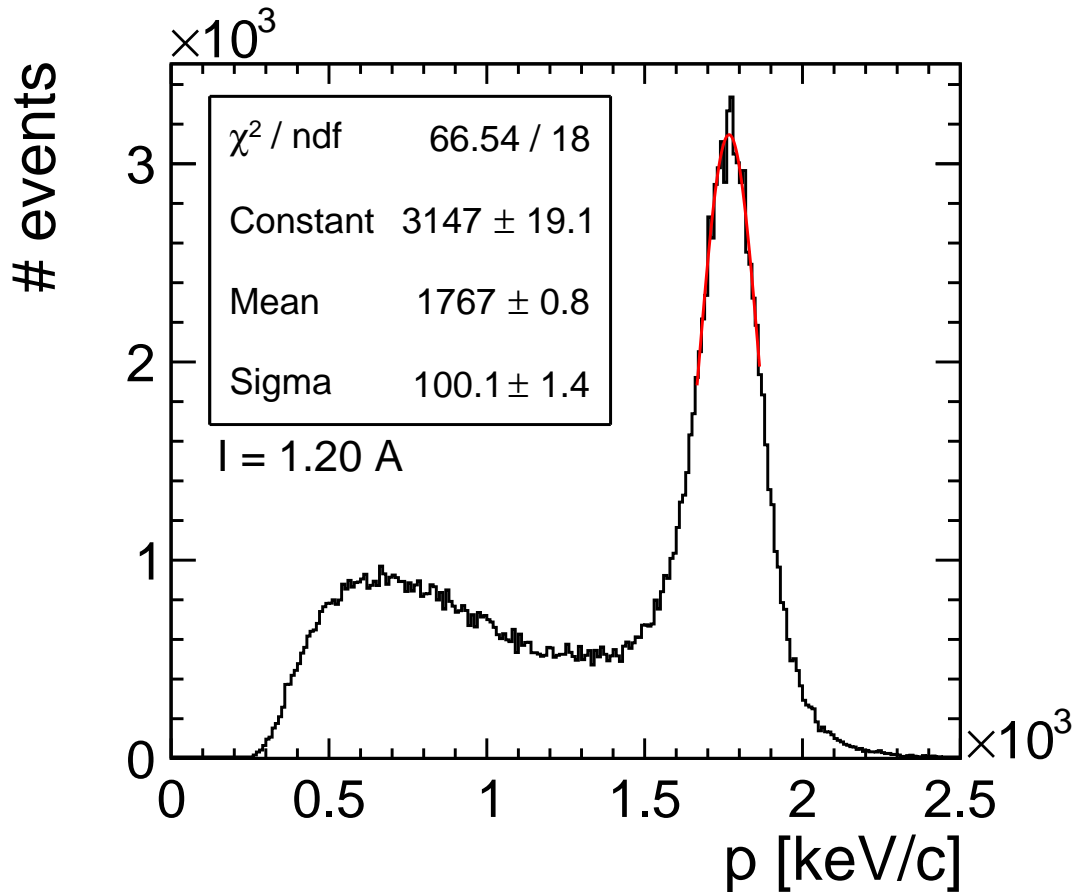


Figure 8: Example of a momentum distribution at a solenoid current of 1.2 A. The red curve is a Gaussian fit that corresponds to the selected electrons. The background corresponds to bremsstrahlung photons escaping the monochromator casing, and is independent of the solenoid current.

selected momentum, may change due to external effects, e.g. if the torque of the screws are modified. For typical applications, the set-up may be used selecting the magnet current which provides the highest rate at the exit of the monochromator. This corresponds to electrons with momenta of about 1.4 - 1.6 MeV/c, i.e. $E \approx 1 \text{ MeV}$. According to Fig. 2 such electrons can be considered as minimum ionising particles.

6. Conclusion

An electron monochromator, based on a high-activity ^{90}Sr source, has been manufactured, assembled, and characterised by using a LYSO crystal coupled to a digital silicon photomultiplier array. After determining the non-linearity of the dSiPM/LYSO response with a ^{22}Na source, a

I [A]	N_{cells}	E [keV]	σ_E [keV]	σ_E/E [%]	p [keV/c]	σ_p [keV/c]	σ_p/p [%]
0.40	1018	248	83	33.5	561	108	19.3
0.60	1839	488	79	16.2	858	90	10.5
0.65	1943	522	79	15.1	898	88	9.8
0.80	2591	760	81	10.7	1164	87	7.5
1.00	3243	1050	88	8.4	1474	92	6.2
1.10	3504	1187	94	8.0	1619	97	6.0
1.15	3594	1237	91	7.4	1672	94	5.6
1.20	3750	1328	96	7.2	1767	100	5.7
1.30	3986	1485	103	6.9	1929	105	5.4
1.40	4138	1594	106	6.6	2042	111	5.4
1.60	4467	1871	108	5.8	2327	108	4.6

Table 1: Measurement results for various solenoid current settings across the ^{90}Sr emission spectrum. E denotes the kinetic energy of the electrons. σ_p corresponds to the width of the Gaussian fit to the peaks for each current. σ_E is calculated by error propagation following eq. 3

study of the electron momentum selection as a function of the solenoid current has been performed. As expected, a linear dependency was observed. Additionally, the resolution of the momentum selection has been measured for various currents. It was shown that a 5 % spread in momentum selection can be achieved for electrons above ~ 2 MeV/c, rendering this device very useful for small laboratory experiments requiring MIPs.

In typical applications, the monochromator will be used in combination with a trigger counter. In the tile scan set-up for the Linear Collider Detector studies, a cross arrangement of two 1 mm thick squared scintillating fibres is mounted in about 1 cm distance from the exit slit. The effective trigger area = 1 mm². The typical trigger rate is of the order 10 Hz.

Acknowledgements

We would like to acknowledge the team at the Institut de Recherches Subatomiques, Strasbourg, France, which designed the electron monochromator. We are grateful to Raphael Dumps, Pierre-Ange Giudici and Ilia Krasin (all CERN) for their competent technical support in producing the components and assembling the source. We thank Abderrahim Errahhaoui from the CERN radioprotection service for the insertion of the ^{90}Sr source into the housing and Felix Bergsma (CERN) for making the Hall probe available. The help of the technical student Cesare Alfieri in some of the measurements was much appreciated. We thank Wolfgang Klempt for his critical reading and constructive suggestions.

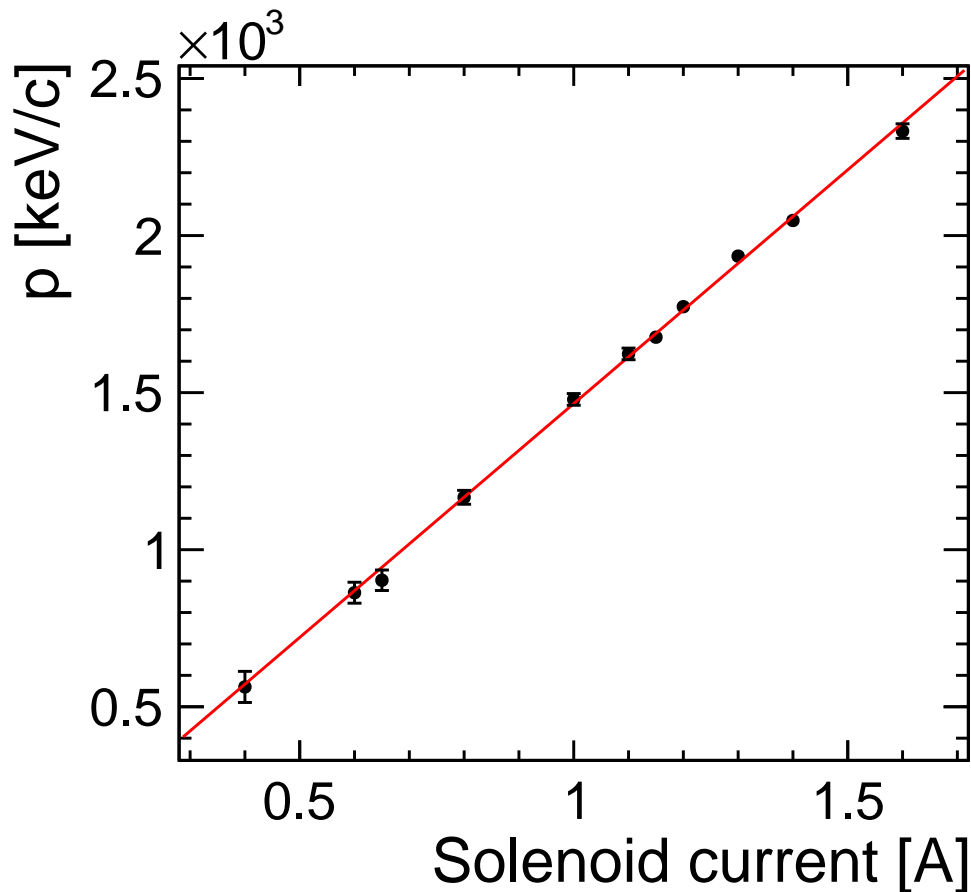


Figure 9: Electron momentum as a function of the electron monochromator solenoid current. The red curve corresponds to a linear fit to the data points.

References

- [1] CALICE Collaboration. CALICE report to the DESY Physics Research Committee, April 2011. [arXiv:1105.0511v2](https://arxiv.org/abs/1105.0511v2).
- [2] J. Marshall and M. A. Thomson. Redesign of the Pandora Particle Flow algorithm, 2010. [Report at the IWLC 2010](#).
- [3] <https://twiki.cern.ch/twiki/bin/view/AXIALPET/WebHome>.
- [4] P. Beltrame, et al. The AX-PET demonstrator - Design, construction and characterization. *Nuclear Instruments and Methods A*, vol. 654(1) pp. 546 – 559, 2011.
- [5] C. Casella, M. Heller, C. Joram, and T. Schneider. A high resolution TOF-PET concept with

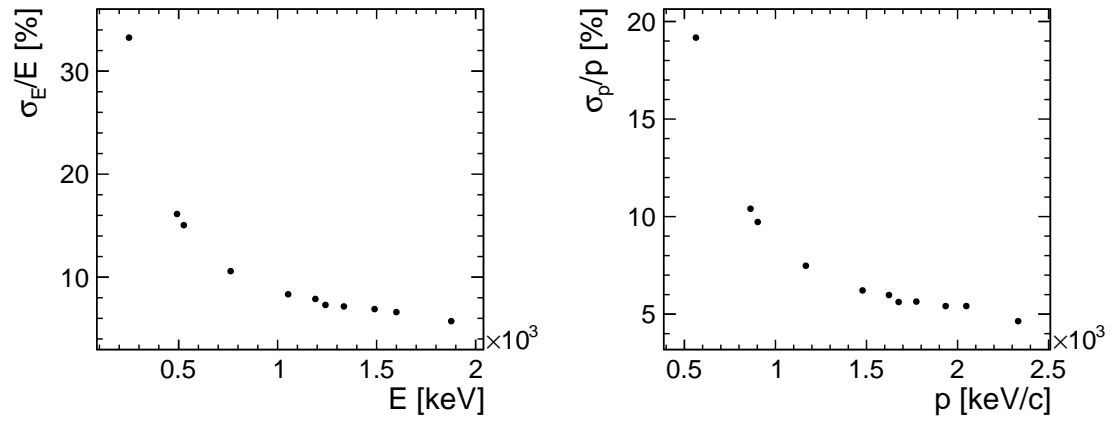


Figure 10: Energy (left) and momentum (right) resolutions for the various solenoid current settings. A momentum selection of $\sim 5\%$ can be achieved for currents above 1.4 A.

axial geometry and digital SiPM readout . *Nuclear Instruments and Methods A*, vol. 736(0) pp. 161 – 168, 2014.

[6] <http://www.digitalphotoncounting.com/tech-details>.

A. Additional figures

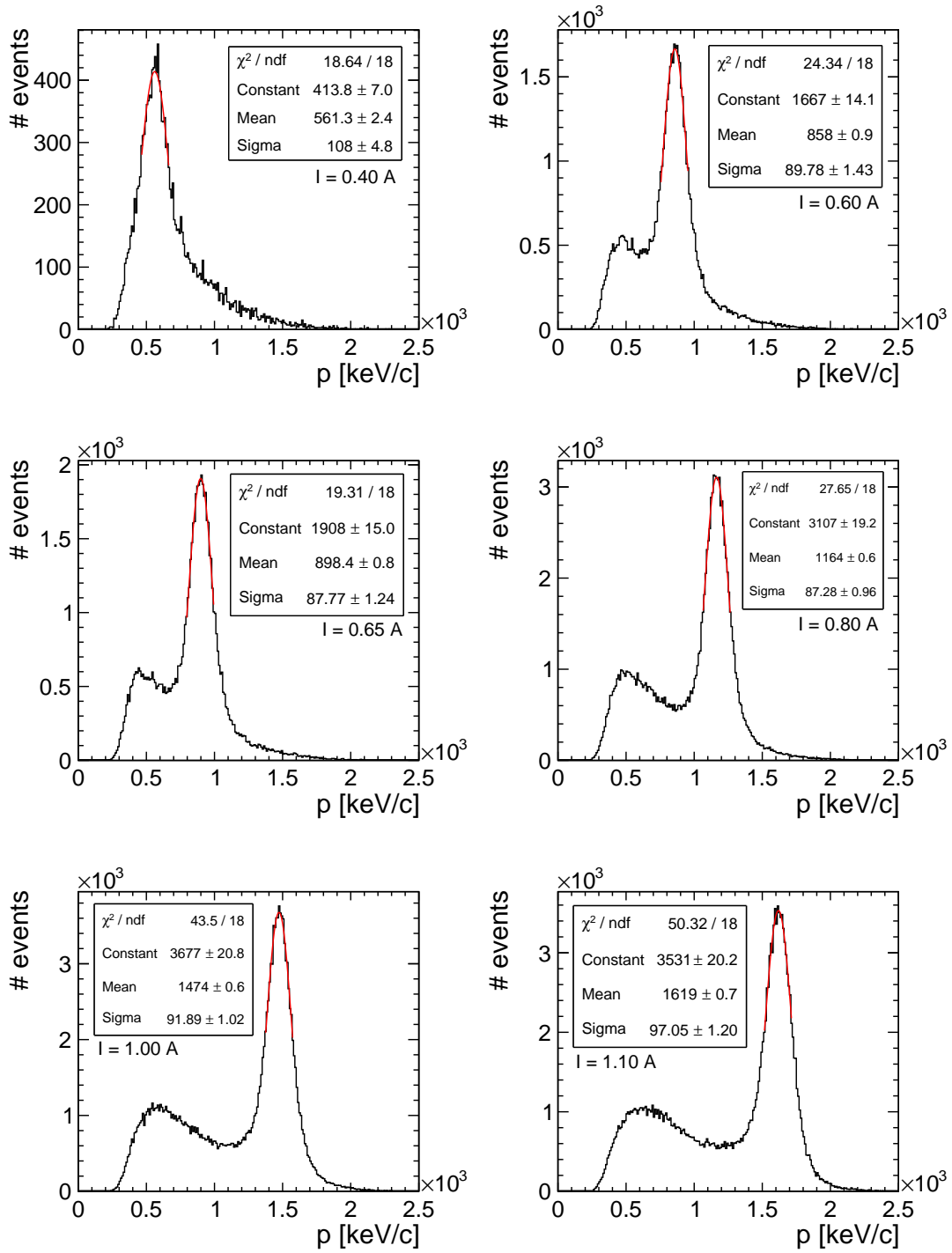


Figure 11: Momentum distributions for various solenoid current values

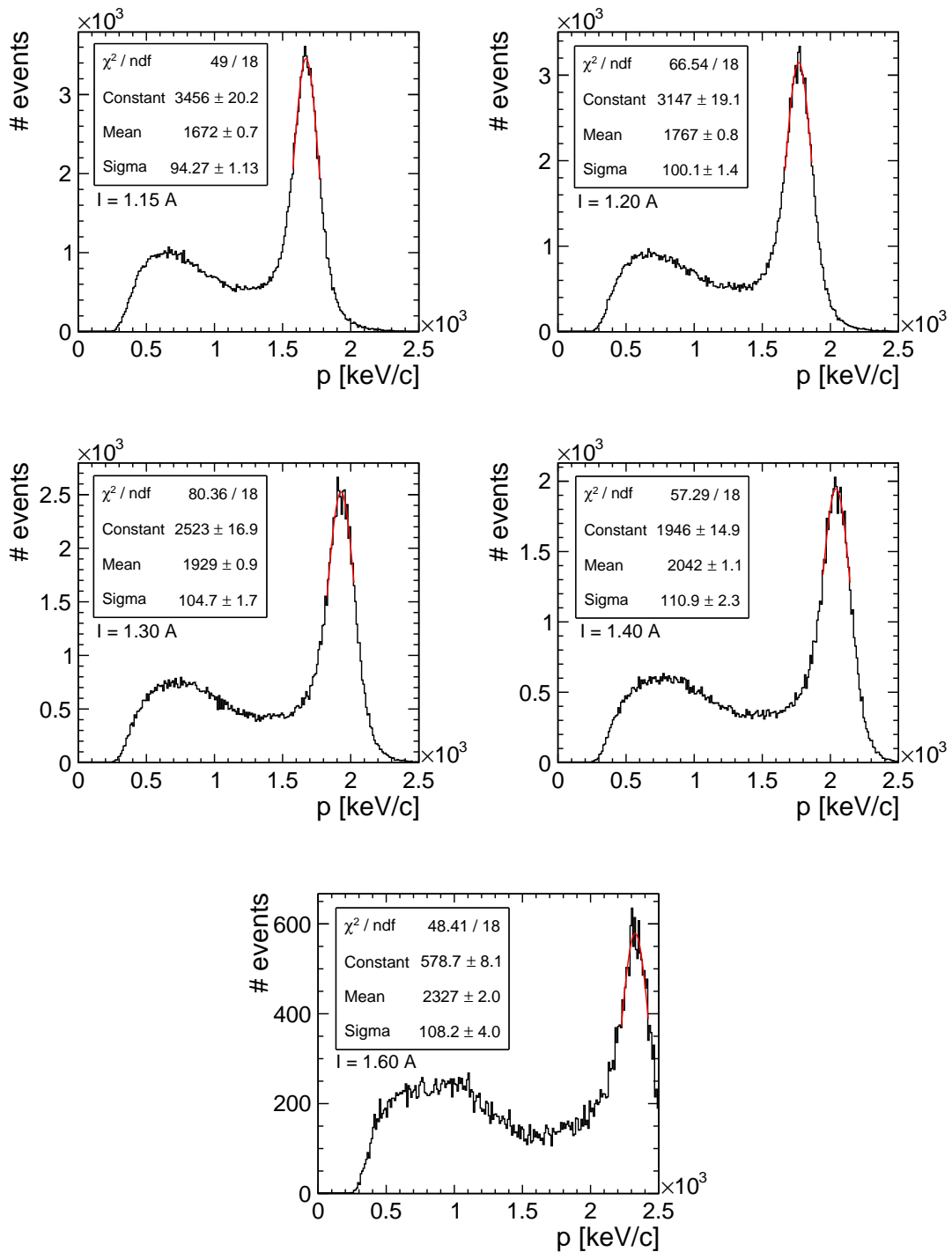


Figure 12: Momentum distributions for various solenoid current values

B. Technical drawings

The technical drawings show the assembly of the SPECTRO A ELECTRONS ENSEMBLE. It includes two cross-sectional views (Ech. 4/1 and Ech. 4/2) showing the internal components and their assembly. The cross-sections are labeled with callouts 1 through 15. The top views show the layout of the components, with callouts 1, 2, 3, 4, 5, 6, 7, 8, 9, 10, 11, 12, 13, 14, and 15. A perspective view shows the external appearance of the device, with callouts 14 and 15.

collimateur 2 montage suivant 7

collimateur 1 montage suivant 8

Ech. 4/1

Ech. 4/2

10	1	Alu.			
11	2	Alu.			13,30 x 4,43
12	3	Vis. C20 M4-20	2000		
13	4	Vis. C20 M4-25	2000		
14	4	Vis. F100 M4-5	2000		
15	1	Alu.			13,30 x 4,43
16	1	Collimateur 2	ENSEMBLE		M 346/019
17	1	Capot	Empose		M 346/022
18	1	Batterie	PVC		M 346/020
19	2	Bornes	TOUL.		M 346/011
20	1	Boite 2	Per AMO3		M 346/036
21	2	Boite 1	Per AMO3		M 346/035
22	1	Collimateur 1	ENSEMBLE		M 346/038
23	1	Alu.			55,10 x 4,43
24	1	Support	TOUL.		M 346/033
25	2	Boite 3	Per AMO3		M 346/037
26	2	Ornifle	TOUL.		M 346/030
27	1	Corps	Empose		M 346/034

REP. NBS. DESIGNATION MATER. OBSERVATION

Rég. gén. : Tal. gén. : Angles charnt. :

ENM

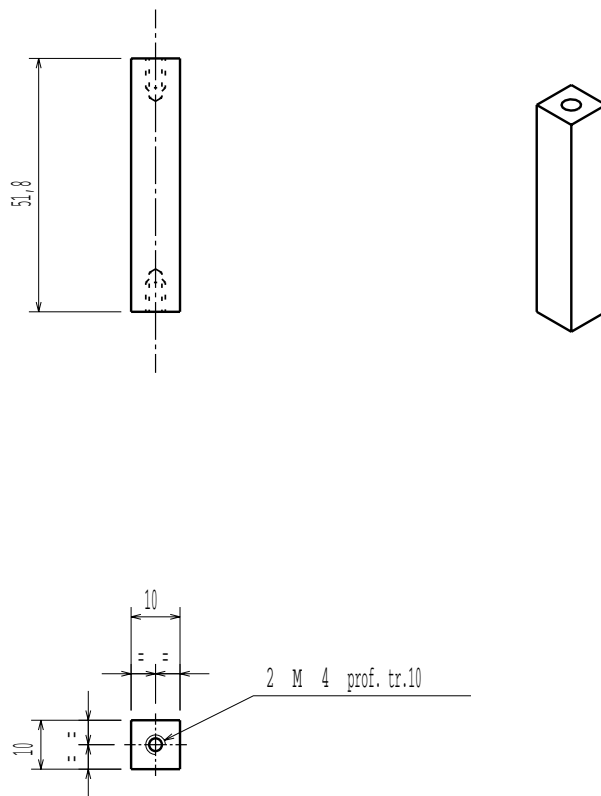
SPECTRO A ELECTRONS ENSEMBLE


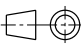
INSTITUT DE RECHERCHES SUBATOMIQUES (base) : PETER R. 12.04.2

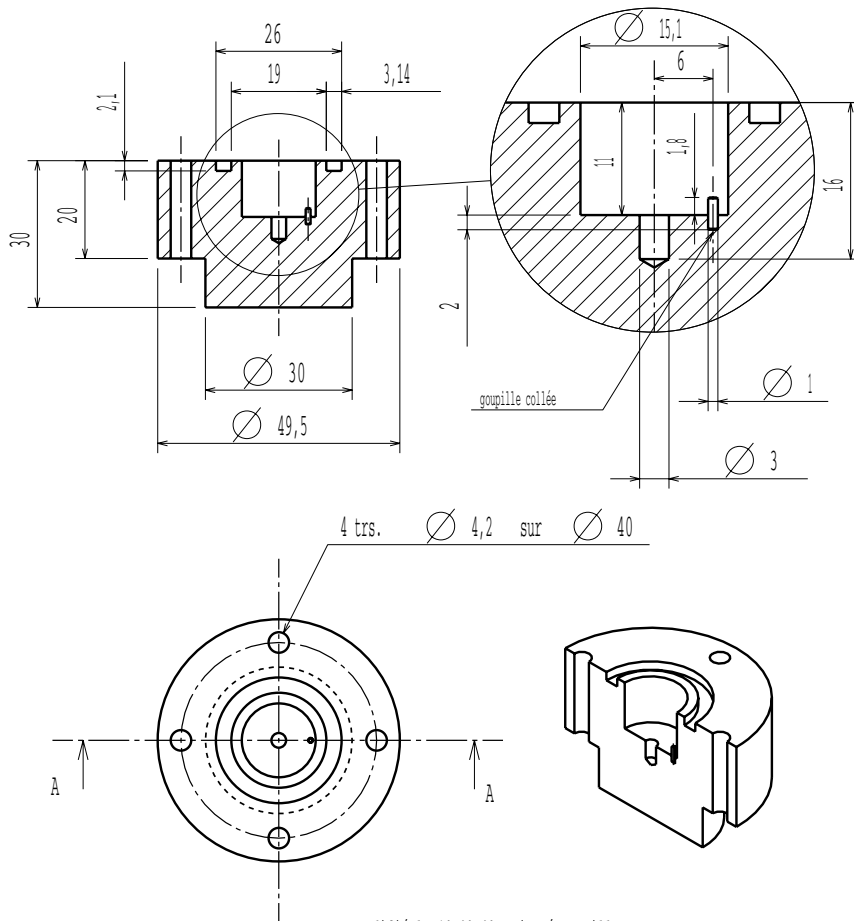
BP.28, 67037 STRASBOURG CEDEX 2 (ven.) : CALLENT J. 1

Formel 246-005

1/1

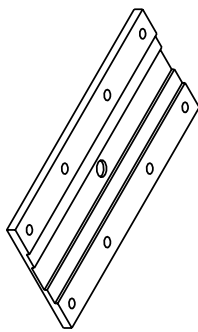
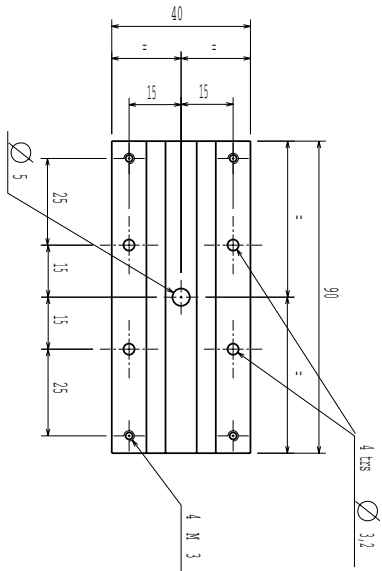
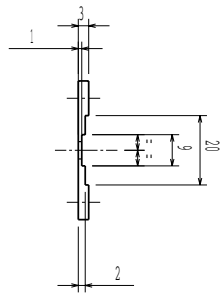


9	2	Carre de 10x10 long.55	DURAL		
REP.	NB.	DESIGNATION	MATIERE	OBSERVATIONS	
Rug. gén.:	Ra 3,2	Tol. gén.:	Js13/js13	Angles, chanf.: 0.2 a 45°	
GIM		<i>SPECTRO A ELECTRONS</i> ENTRETOISE			
 <small>IN2P3</small> <small>ULP</small>	INSTITUT DE RECHERCHES SUBATOMIQUES		Dess.:	PETER R.	11.04.2001
	BP.28, 67037 STRASBOURG CEDEX 2		Véri.:	CAILLERET J.	
Echelle		Format	246-011		
1/1		A4			




a modifié le 18 03 03 ajouté goupille

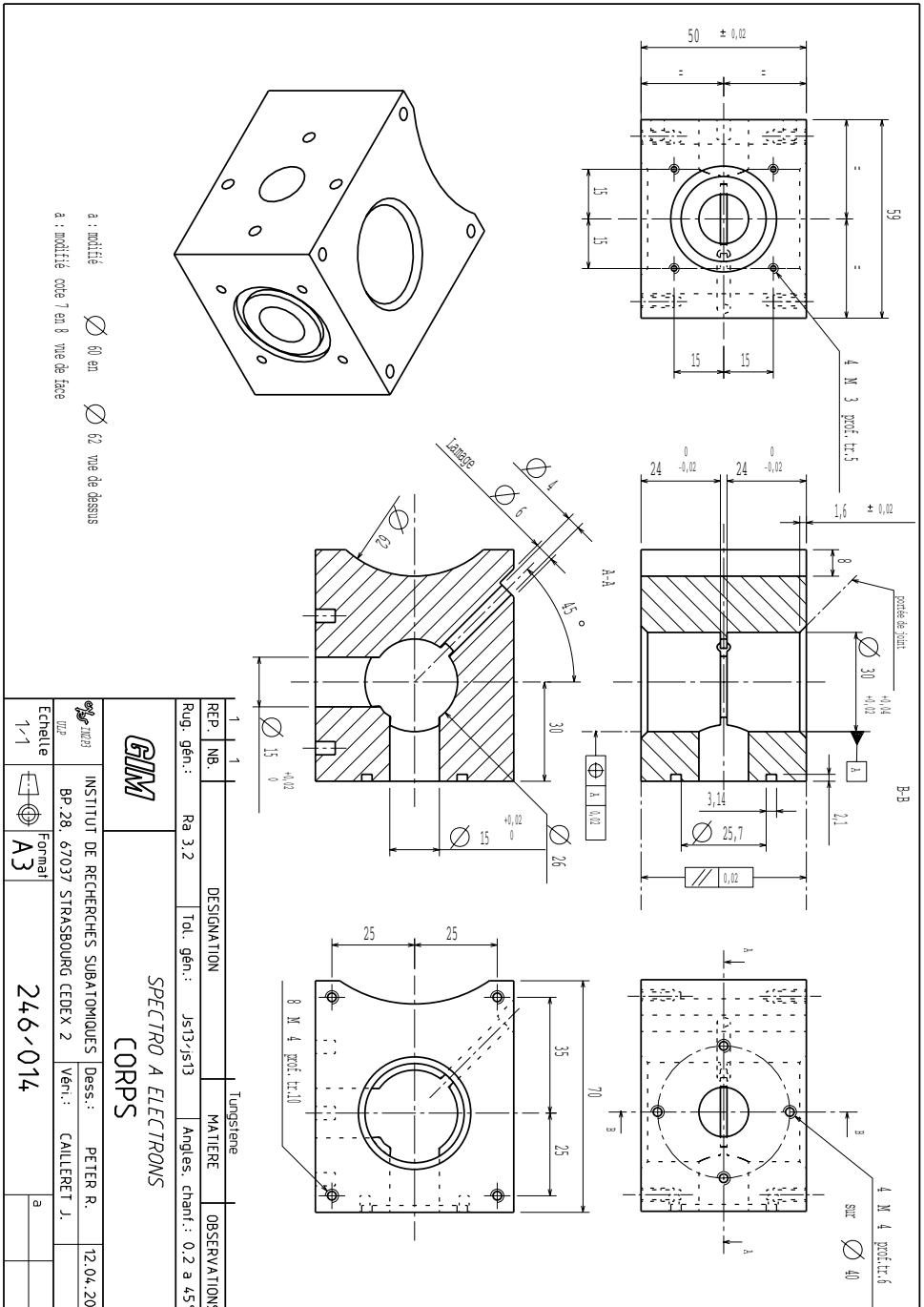
11	1	Rondin \varnothing 50	Tungstene	
REP.	NB.	DESIGNATION	MATIERE	OBSERVATIONS
Rug. gén.:	Ra 3,2	Tol. gén.:	Js13/js13	Angles, chanf.: 0.2 a 45°
GIM		<i>SPECTRO A ELECTRONS</i> CAPOT		
IN2P3	INSTITUT DE RECHERCHES SUBATOMIQUES		Dess.:	PETER R.
ULP	BP.28. 67037 STRASBOURG CEDEX 2		Véri.:	CAILLERET J.
Echelle		Format		
1/1		A4	246-012	
			a	



modifié le 20.04.03

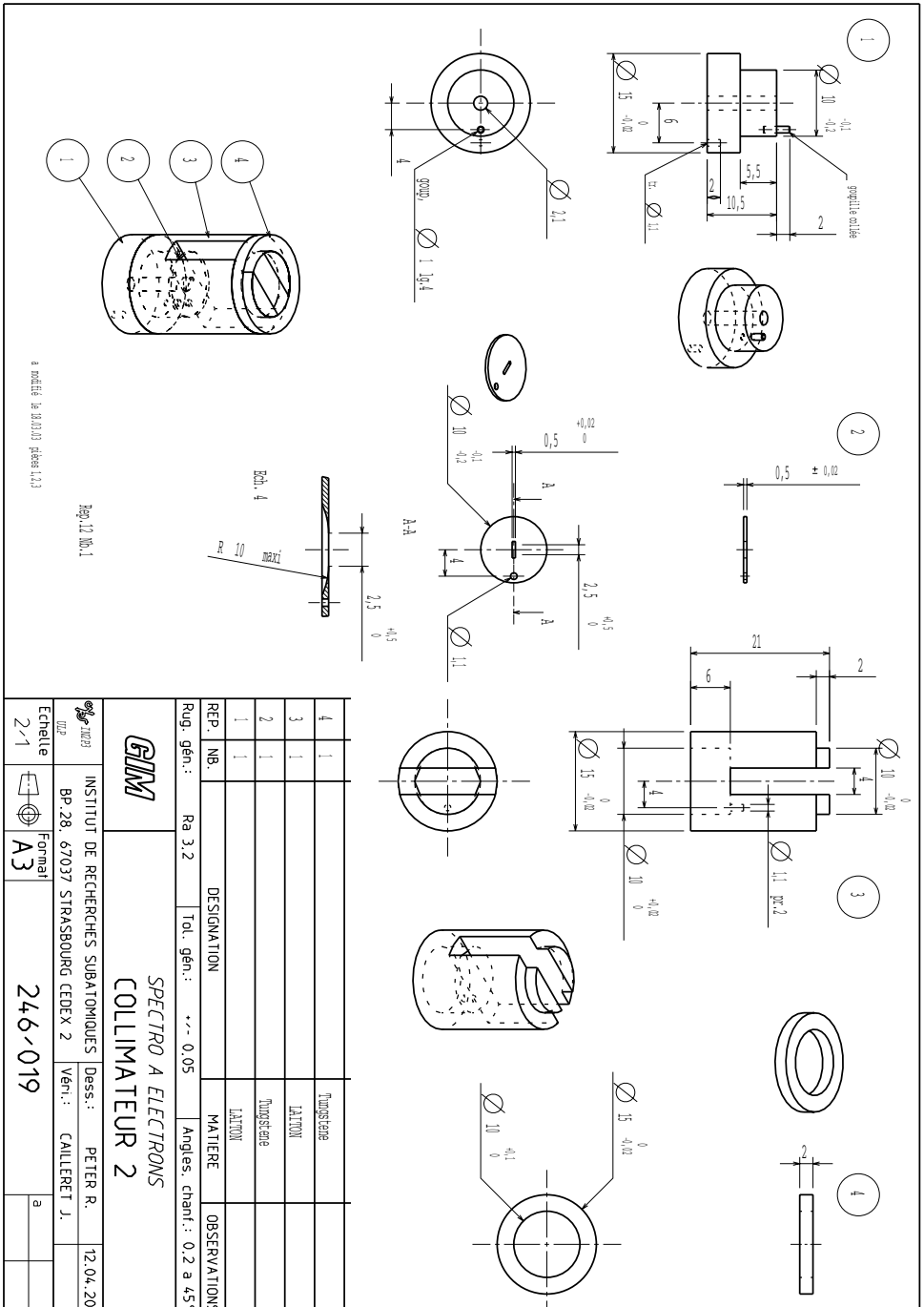
4 tirs. \varnothing 3,2
4 M3

REP. NB.:	4	1	1						
Rug. gén.:	Ra 3.2		Tol. gén.:		J513/j513		Matière:		DURAL
			SPECTRO A ELECTRONES SUPPORT						
INSTITUT DE RECHERCHES SUBATOMIQUES BP. 28. 67037 STRASBOURG CEDEX 2			Dess.: PETER R.		Verif.: CALLIERT J.		11.04.2001		
Echelle:	1/1	Formal:	A3						
246-013									






a : modifié
 a : modifié entre 7 en 8 vue de face

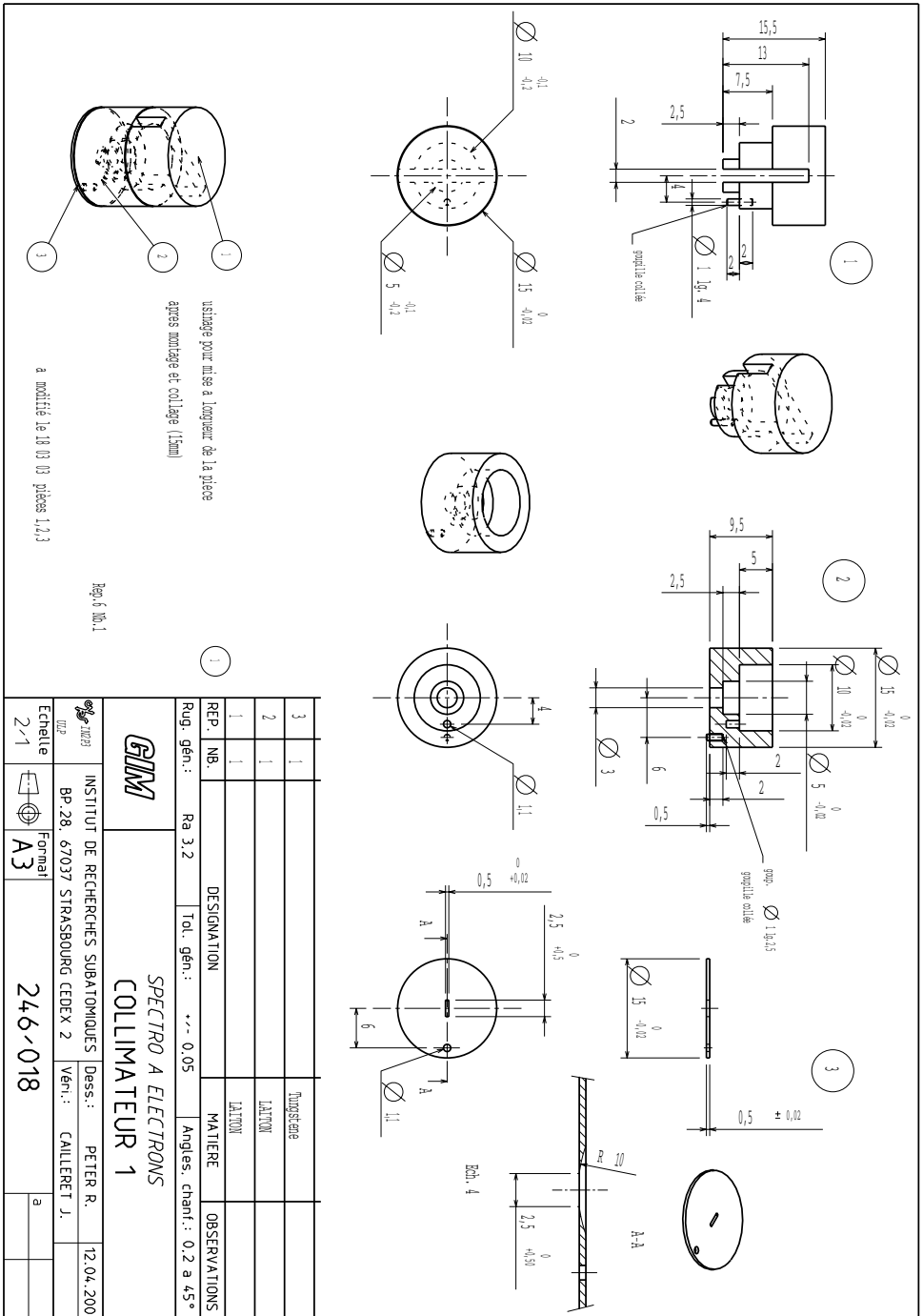
REP. NB.:	1	1	DESIGNATION	Tungstene	MATIERE	OBSERVATIONS
Rug. gén.:	Ra 3.2	Tol. gén.:	J513/J513	Angles. chanf.:	0.2 a 45°	
			SPECTRO A ELECTRONICS CORPS			
INSTITUT DE RECHERCHES SUBATOMIQUES BP 28 67037 STRASBOURG CEDEX 2		Dess.: PETER R. Ven.: CALLETET J.		12.04.2001		
Echelle	1/1	Formai	A3	a		
246-014						



8 modifié de H.03.03 page 12.3

Rep. 12. Nb. 1

REP. 1	NB. 1	DESIGNATION	MATIERE	OBSERVATIONS
4	1	Duogéomé		
3	1	LATON		
2	1	Duogéomé		
1	1	LATON		
Rug. gén. :		Ra 3.2	Tol. gén. : +- 0.05	
			Angles. chanf. : 0.2 a 45°	
 SPECTRO A ELECTRONES COLLIMATEUR 2				
 INSTITUT DE RECHERCHES SUBATOMIQUES BP. 28. 67037 STRASBOURG CEDEX 2		Dess. : PETER R. Verif. : CALLIERT J.	12.04.2001	
Echelle	 2-1	Format A3	a	
246-019				



usage pour mise à l'ouvrage de la pièce
après montage et collage (15mm)

à modifier le 18 03 03 pièces 1,2,3

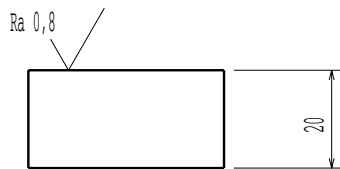
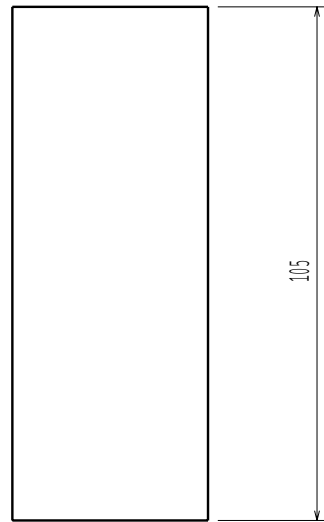
Fig. 6 Mod. 1

REP	NB.	DESIGNATION	MATIERE	OBSERVATIONS
1	1		LAITON	
2	1		LAITON	
3	1		Diversifiée	

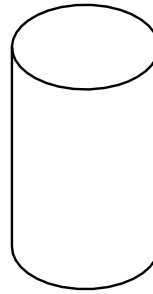
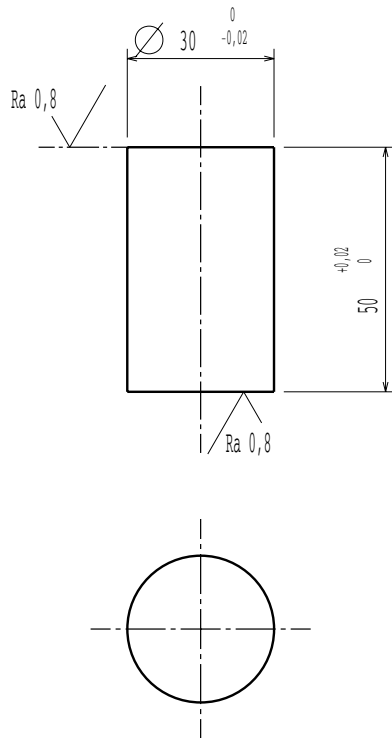
Rug. gén.:	Ra 3.2	Tol. gén.:	*** 0.05	Angles. charf.:	0.2 à 45°
------------	--------	------------	----------	-----------------	-----------

GIM		SPECTRO A ELECTRONS	
COLLIMATEUR 1			
INSTITUT DE RECHERCHES SUBATOMIQUES	DESS.:	PETER R.	12.04.2001
BP. 28. 67037 STRASBOURG CEDEX 2	VEN.:	CALLIET J.	

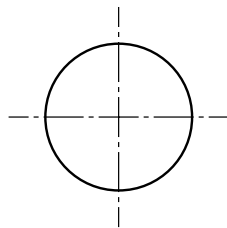
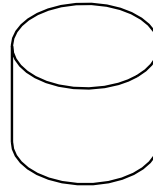
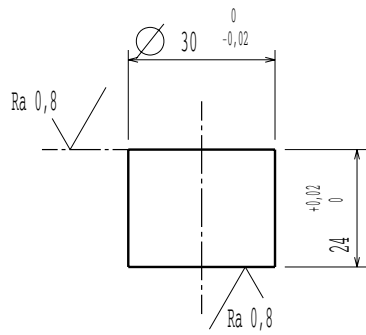
Echelle	2-1	Formai	A3	a
---------	-----	--------	----	---



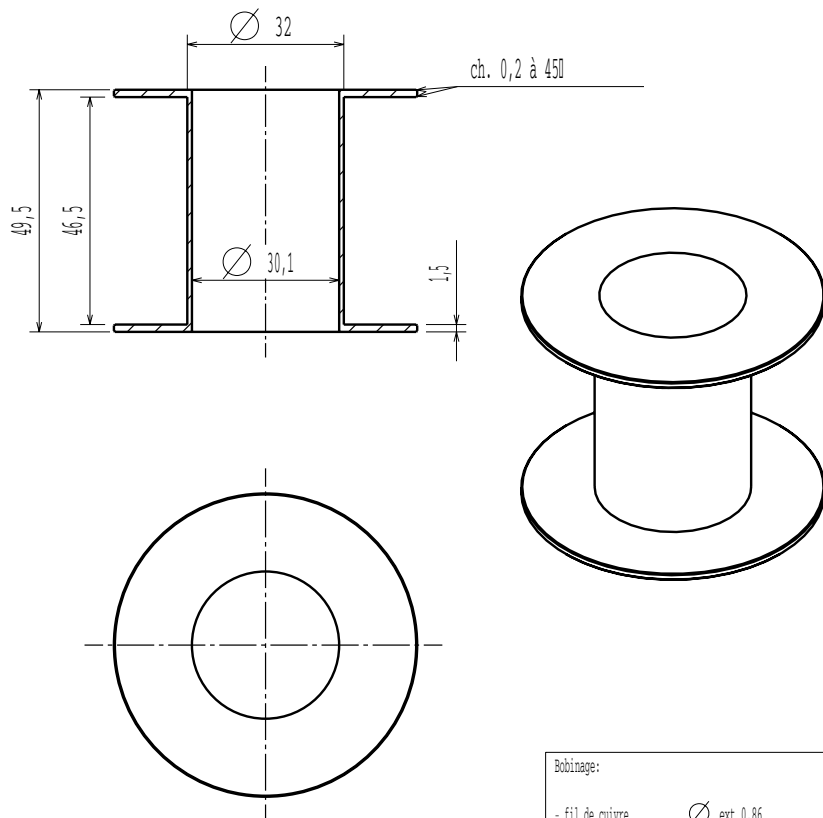
3	2			Fer ARMCO	
REP.	NB.	DESIGNATION	MATIERE	OBSERVATIONS	
Rug. gén.:	Ra 3,2	Tol. gén.:	Js13/js13	Angles. chanf.: 0.2 a 45°	
GIM		<i>SPECTRO A ELECTRONS</i> POLE 3			
 IN2P3 ULP	INSTITUT DE RECHERCHES SUBATOMIQUES		Dess.:	PETER R.	12.04.2001
	BP.28. 67037 STRASBOURG CEDEX 2		Véri.:	CAILLERET J.	
Echelle 1/1		Format A4	246-017		



8	1	Fer ARMCO	
REP.	NB.	DESIGNATION	OBSERVATIONS
Rug. gén.:	Ra 3,2	Tol. gén.:	Js13/js13 Angles. chanf.: 0.2 a 45°
GIM		<i>SPECTRO A ELECTRONS</i> POLE 2	
 IN2P3 ULP	INSTITUT DE RECHERCHES SUBATOMIQUES		Dess.: PETER R. 12.04.2001
	BP.28. 67037 STRASBOURG CEDEX 2		Véri.: CAILLERET J.
Echelle 1/1		Format A4	246-016



7	2	Fer ARMCO	
REP.	NB.	DESIGNATION	OBSERVATIONS
Rug. gén.:	Ra 3,2	Tol. gén.:	Js13/js13 Angles. chanf.: 0.2 a 45°
GIM	<i>SPECTRO A ELECTRONS</i> POLE 1		
 <small>IN2P3</small> <small>ULP</small>	INSTITUT DE RECHERCHES SUBATOMIQUES		Dess.: PETER R.
	BP.28. 67037 STRASBOURG CEDEX 2		Véri.: CAILLERET
Echelle 1/1		Format A4	246-015



indice a 10.10.2005:
 Ø 60 devient
 Ø 30,2 devient
 ep.2 devient 1,5
 45,5 devient 46,5

Ø 62
 Ø 30,1

Bobinage:
 - fil de cuivre Ø ext 0,86
 (Ø int= 0,80mm)
 - minimum 16 couches de 52 spires
 - à bobiner couche par couche

10	1	PVC			
REP.	NB.	DESIGNATION	MATIERE	OBSERVATIONS	
Rug. gén.:	Ra 3,2	Tol. gén.:	Js13/js13	Angles. chanf.: 0.2 a 45°	
GIM		<i>SPECTRO A ELECTRONES</i> BOBINE			
IN2P3	INSTITUT DE RECHERCHES SUBATOMIQUES		Dess.:	PETER R.	12.04.2001
ULP	BP.28. 67037 STRASBOURG CEDEX 2		Véri.:	CAILLERET J.	
Echelle		Format	246-020		a
1/1		A4			